Analysis of the plasticity regions in elastoplastic torsion problem using mixed complementarity algorithm

Tatiana D. Assis[1], Sandro R. Mazorche[1]

[1]*Dept. of Mathematics, Federal University of Juiz de Fora*
University campus, CEP 36.036-330, Juiz de Fora/MG, Brazil
tatiana.danelon@engenharia.ufjf.br, sandro.mazorche@ufjf.edu.br

Abstract. The elastoplastic torsion problem (ETP) consists of defining portions of elasticity and plasticity in the cross section of a bar twisted by terminal couples. This problem can be modelled by using variational principles and is considered an obstacle type problem by means of the membrane analogy. At points where the membrane touches the obstacle, permanent deformations ensues. Thus, the problem can be rewritten as a mixed complementarity problem and solved using the FDA-MNCP algorithm (Feasible Directions Algorithm for Mixed Nonlinear Complementarity Problem). In this work, the objective is to analyze the influence of the shape of the cross section in the resulting regions of plasticity. Some numerical simulations were made for different rectangular proportions, with the fixed area, to observe how the shape of these regions varies and the percentage they represent in relation to the total area. In addition, the plastic portions were compared for three sections of the same area and material, in the formats: disk, square and L.

Keywords: Obstacle problem, Elastoplastic torsion, Complementarity problem, Finite difference method.

1 Introduction

As a result of applied loading's, elastic solids will change shape or deform. The elastoplastic material behavior is defined by the strain decomposition in the elastic and plastic parts. Thus, the elastoplastic torsion problem (ETP) consists of defining portions of elasticity and plasticity in the cross section of a bar twisted by terminal couples. Originally, the set of admissible displacements is given in terms of gradient norm for displacements ($\mathcal{K}_\nabla$). In this case, the numerical resolution has been more explored using the finite element method, as can be seen in Dolan et al. [1]. The equivalence proved by Brezis and Sibony [2] was a milestone in the area as it enabled the rewrite of the ETP to a more convenient set $\mathcal{K}_d$, using the distance to the boundary (d). The problem in this formulation is especially appropriate for a numerical solution by using the finite difference method (FDM), because is more easy to implement numerically. With this approach, the ETP can be regarded as an obstacle type problem by means of the membrane analogy.

The objective of this work is to analyze the influence of the cross section in the resulting plastic zones. All the simulations were performed for two cases: (i) different rectangular sections with the same area; (ii) circular, square and L-sections with the same area. The elastoplastic torsion problem is described as a mixed complementarity problem, which is solved by using FDA-MNCP (feasible directions algorithm mixed nonlinear complementarity problems), proposed by Gutierrez et al. [3]. Thus, the results obtained allow to analyze the boundary of the plastic zones and the percentage they represent in relation to the total area.

2 Elastoplastic torsion problem

Consider an elastic cylinder bar, with a simply connected cross section $\Omega \subset \mathrm{R}^2$, subjected to a torsion applied at the ends and with the lateral boundary stress-free. This cylindrical body is a prismatic bar isotropic and homogeneous, with constant cross section. Under torque T, the displacement of a generic point P in the xy-plane will move to location P', causing the line segment $\overline{OP}$ to rotate at an angle β. The displacement of each point of

the twisted bar, in the xy-plane, can thus be determined as:

$$w_x = -r\beta \sin(\alpha) = -\beta y, \qquad w_y = r\beta \cos(\alpha) = \beta x, \tag{1}$$

where $r = \|\overrightarrow{OP}\|$ and α is the angle between the line segment $\overline{OP}$ and the x-axis. Using the assumption that the section rotation is a linear function of the axial coordinate, we can assume that the cylinder is fixed at $z = 0$ and take $\beta = \theta z$, where θ is the angle of twist per unit length. Therefore:

$$w_x = -\theta yz, \qquad w_y = \theta xz, \qquad w_z = \theta\zeta(x, y), \tag{2}$$

where $\zeta = \zeta(x, y)$ is a function that describes the out-of-plane displacement.

Thus, the following stress tensor is obtained:

$$\sigma = \begin{bmatrix} 0 & 0 & \mu\theta\left(\frac{\partial\zeta}{\partial x} - y\right) \\ 0 & 0 & \mu\theta\left(\frac{\partial\zeta}{\partial y} + x\right) \\ \mu\theta\left(\frac{\partial\zeta}{\partial x} - y\right) & \mu\theta\left(\frac{\partial\zeta}{\partial y} + x\right) & 0 \end{bmatrix}, \tag{3}$$

it means, only $\tau_{xz} = \tau_{zx}$ and $\tau_{yz} = \tau_{zy}$ are nonzero. Applying these stresses in the equilibrium equations with zero body forces $\frac{\partial\tau_{xz}}{\partial x} + \frac{\partial\tau_{yz}}{\partial y} = 0$. So, taking

$$\tau_{xz} = \frac{\partial\varphi}{\partial y}, \qquad \tau_{yz} = -\frac{\partial\varphi}{\partial x}, \tag{4}$$

the equilibrium is satisfied, where $\varphi = \varphi(x, y)$ is the Prandtl stress function. Poisson's equation is also satisfied by φ. Indeed, as $\tau_{xz} = \mu\theta\left(\frac{\partial\zeta}{\partial x} - y\right)$ and $\tau_{yz} = -\mu\theta\left(\frac{\partial\zeta}{\partial y} + x\right)$, one has:

$$\Delta\varphi = \frac{\partial^2\varphi}{\partial x^2} + \frac{\partial^2\varphi}{\partial y^2} = -2\mu\theta. \tag{5}$$

Also, the stress-free condition on the lateral boundary of the cylinder, can be rewritten as:

$$\frac{d\varphi}{ds} = 0, \tag{6}$$

where s denotes the curvilinear abscissa. So, φ must be constant along $\partial\Omega$ because Ω is a simply connected section and eq. (4) defines φ inside a constant, one takes $\varphi = 0$ in $\partial\Omega$.

The effective or von Mises stress will be used, considering a elastic-perfectly plastic material. According to Sadd [4], this stress is given by the expression:

$$\sigma_e = \tfrac{1}{\sqrt{2}}\left[(\sigma_x - \sigma_y)^2 + (\sigma_y - \sigma_z)^2 + (\sigma_z - \sigma_x)^2 + 6(\tau_{xy}^2 + \tau_{yz}^2 + \tau_{zx}^2)\right]^{1/2}. \tag{7}$$

In ETP, only τ_{xz} and τ_{yz} are nonzero, thus eq. (7) can be rewritten as:

$$\sigma_e = \sqrt{3(\tau_{yz}^2 + \tau_{zx}^2)} = \sqrt{3}||\nabla\varphi||. \tag{8}$$

Let γ' be the yield limit (threshold of plasticity) for a material, taking $\gamma = \frac{\sqrt{3}}{3}\gamma'$ the cross section is divided into two regions:

$$P = \{||\nabla\varphi|| = \gamma\} = \{\texttt{plastic zone}\}, \qquad E = \{||\nabla\varphi|| < \gamma\} = \{\texttt{elastic zone}\}. \tag{9}$$

2.1 Variational inequality formulation

As detailed in Rodrigues [5], the complementary energy involved in the elastoplastic problem is given by:

$$J(\varphi) = \frac{l}{2\mu}\int_\Omega ||\nabla\varphi||^2\, dxdy - 2\theta l\int_\Omega \varphi\, dxdy. \tag{10}$$

Thus, the principle of minimum complementary energy leads to the variational problem:

$$\varphi \in \mathcal{K}_\gamma :\ J(\varphi) \le J(\eta)\ \ \forall\eta \in \mathcal{K}_\gamma, \tag{11}$$

or equivalently:

$$\varphi \in \mathcal{K}_\gamma : \int_\Omega \nabla\varphi \cdot \nabla(\eta - \varphi)\, dxdy \geq 2\mu\theta \int_\Omega (\eta - \varphi)\, dxdy, \quad \forall \eta \in \mathcal{K}_\gamma, \tag{12}$$

where $\mathcal{K}_\gamma = \{\eta \in V : \ ||\nabla\eta|| \leq \gamma \ \texttt{in}\ \Omega,\ \eta = 0 \ \texttt{on}\ \partial\Omega\}$.

The PTE is a special case of an obstacle type problem, which is an important application of elliptic variational inequalities and the basis for formulation of many physical phenomena. In its classical form, the obstacle problem considers an elastic membrane in $\Omega \subset R^2$ equally stretched in all directions by a uniform tension and loaded by a normal uniformly distributed force f. Let $g(x, y)$ be the function that prescribes the displacement on the $\partial\Omega$ boundary, the equilibrium position of the membrane can be stated by the Poisson problem:

$$\begin{aligned} \Delta u &= -f \ \texttt{in}\ \Omega, \\ u &= g \ \texttt{on}\ \partial\Omega. \end{aligned} \tag{13}$$

This is the simple case, representing a free membrane. Now, one introduces an obstacle d satisfying $d \geq 0$ in $\partial\Omega$, which forces the membrane to lie below the rigid body $\left\{(x, y, z) \in R^3 : z \leq d(x, y)\right\}$.

Let $d : \Omega \to \mathrm{R}$ the distance of $(x, y) \in \Omega$ to the boundary $\partial\Omega$, define:

$$u = -\frac{\varphi}{\gamma}, \quad c = \frac{2\mu\theta}{\gamma}, \quad g = 0, \tag{14}$$

where θ is the angle of twist per unit length, μ is the modulus of rigidity and $\gamma > 0$ is the threshold of plasticity. With this equivalence the plastic (P) and the elastic (E) zones may also be given, respectively, by:

$$P = \{||\nabla u|| = 1\} = \{u = d\}\,, \qquad E = \{||\nabla u|| < 1\} = \{u < d\}\,. \tag{15}$$

Therefore, from eq. (12) we obtain the following variational inequality:

$$u \in \mathcal{K}_\nabla : \int_\Omega \nabla u \cdot \nabla(v - u)\, dxdy \geq -c \int_\Omega \nabla(v - u)\, dxdy, \quad \forall v \in \mathcal{K}_\nabla, \tag{16}$$

where $\mathcal{K}_\nabla = \left\{v \in \mathcal{H}_0^1(\Omega) : ||\nabla v|| \leq 1 \ \ a.e.\ \texttt{in}\ \Omega\right\}$.

To find the solution in $\mathcal{K}_\nabla$ it is necessary to approximate the gradient norm, which can be complex. Then define a more convenient set $\mathcal{K}_d = \left\{v \in \mathcal{K} : \mathcal{H}_0^1(\Omega) : v(x, y) \leq d(x, y) \ \ a.e.\ \texttt{in}\ \Omega\right\}$ and the problem becomes:

$$u \in \mathcal{K}_d : \int_\Omega \nabla u \cdot \nabla(v - u)\, dxdy \geq -c \int_\Omega \nabla(v - u)\, dxdy, \quad \forall v \in \mathcal{K}_d. \tag{17}$$

The equivalence between eq. (16) and (17) is proved by Brezis and Sibony [2] and Rodrigues [5].

2.2 Mixed complementarity problem

Let $F : \mathcal{D} \subset \mathrm{R}^n \to \mathrm{R}^n \times \mathrm{R}^m$ and $Q : \mathcal{D} \subset \mathrm{R}^m \to \mathrm{R}^n \times \mathrm{R}^m$ vector functions, the mixed complementarity problem (MCP) is defined as finding $(x, y) \in \mathrm{R}^n \times \mathrm{R}^m$ such that:

$$x \geq 0, \ \ F(x, y) \geq 0 \ \ \texttt{and} \ \ \begin{cases} x \bullet F(x, y) = 0 \\ Q(x, y) = 0 \end{cases}, \tag{18}$$

where:

$$x \bullet F(x) = \begin{pmatrix} x_1 F_1(x) \\ \vdots \\ x_n F_n(x) \end{pmatrix}, \tag{19}$$

represents the Hadamard product.

The eq. (17) leads to the mixed complementarity problem:

$$\begin{cases} -\Delta u(x, y) + c &= 0, \quad \texttt{if}\ -d(x, y) < u(x, y) < d(x, y), \\ -\Delta u(x, y) + c &> 0, \quad \texttt{if}\ u(x, y) = -d(x, y), \\ -\Delta u(x, y) + c &< 0, \quad \texttt{if}\ u(x, y) = d(x, y). \end{cases} \tag{20}$$

3 Finite difference model

Solving numerically the PTE as a mixed complementarity problem requires the discretization by using the FDM of the Laplacian solution. In general, for $\Delta u = f$, one has:

$$\frac{\partial^2 u}{\partial x^2}(x_i, y_j) + \frac{\partial^2 u}{\partial y^2}(x_i, y_j) = f(x_i, y_j), \tag{21}$$

where $u(x_i, y_j)$ is the value of the solution at a generic point (x_i, y_j) of the mesh and $i = 0, 1, ..., N_x$, $j = 0, 1, ..., N_y$. Next, this discretization will be presented briefly for rectangular and circular sections. The section in L can be divided into rectangles, with some peculiarities due to it corners. More details for this case can be seen in Danelon [6].

3.1 Rectangular cross section

For a rectangular section, the dimensions k_1, k_2 and the number of mesh points N_x, N_y are variable. The distance between grid points in the x and y directions is given by $h_x = k_1/(N_x - 1)$ and $h_y = k_2/(N_y - 1)$, respectively. Using the centered difference method, the derivatives are approximated by:

$$\frac{\partial^2 u}{\partial x^2}(x_i, y_j) \cong \frac{u(x_i + h_x, y_j) - 2u(x_i, y_j) + u(x_i - h_x, y_j)}{h_x^2}, \tag{22}$$

$$\frac{\partial^2 u}{\partial y^2}(x_i, y_j) \cong \frac{u(x_i, y_j + h_y) - 2u(x_i, y_j) + u(x_i, y_j - h_y)}{h_y^2}. \tag{23}$$

$i = 1, 2, ..., N_x - 1$, $j = 1, 2, ..., N_y - 1$. Replacing the eq. (22) and (23) in eq. (21), one obtains:

$$\frac{U_{i+1,j} - 2U_{i,j} + U_{i-1,j}}{h_x^2} + \frac{U_{i,j+1} - 2U_{i,j} + U_{i,j-1}}{h_y^2} = f_{i,j}, \tag{24}$$

where $U_{i,j}$ denotes the approximate solution of $u(x_i, y_j)$. For $U_{0,j}$, $U_{i,0}$, $U_{N_x,j}$ and U_{i,N_y}, the Dirichlet boundary condition holds.

3.2 Circular cross section

Let the disk of radius R $\Omega = \left\{(x, y) : x^2 + y^2 < R\right\}$. Applying the polar coordinate transformation $x = r\cos\theta$ and $y = r\sin\theta$, where $r = \sqrt{x^2 + y^2}$ and $\theta = \arctan(y/x)$, then eq. (21) becomes:

$$\frac{\partial^2 u}{\partial r^2}(r_i, \theta_j) + \frac{1}{r}\frac{\partial u}{\partial r}(r_i, \theta_j) + \frac{1}{r^2}\frac{\partial u^2}{\partial \theta^2}(r_i, \theta_j) = f(r_i, \theta_j), \qquad 0 < r < R,\ 0 \leq \theta < 2\pi. \tag{25}$$

The eq. (25) has an singularity at the origin caused by the representation of the governing equation in the polar coordinate system. A simple approach to solve this problem is presented by Lai [7], by manipulating the grid point locations. The grid is choosen such that the grid points are half-integered in the radial direction and integered in the azimuthal direction, that is, $r_i = (i - 1/2)\, h_r$ and $\theta_j = (j - 1)h_\theta$, where $h_r = R/(N_r + 1/2)$ and $h_\theta = 2\pi/N_\theta$, $i = 1, 2, ..., N_r + 1$, $j = 1, 2, ..., N_\theta + 1$.

Using the centered difference method to discretize eq. (25), for $i = 2, 3, ..., N_r$, $j = 1, 2, ..., N_\theta$, one has:

$$\Delta u(r_i, \theta_j) \approx \frac{U_{i+1,j} - 2U_{i,j} + U_{i-1,j}}{h_r^2} + \frac{1}{r_i}\frac{U_{i+1,j} - U_{i-1,j}}{2h_r} + \frac{1}{r_i^2}\frac{U_{i,j+1} - 2U_{i,j} + U_{i,j-1}}{h_\theta^2}. \tag{26}$$

The boundary values are given by $U_{N_r+1,j} = 0$ and $U_{i,N_\theta+1} = U_{i,1}$, because U is 2π periodic in θ. At $i = 1$, the coefficient $U_{0,j}$ is zero, because $r_1 = h_r/2$. Therefore, the scheme does not need any pole condition.

4 Numerical results

The angle of rotation, present in the physical constant c, depends on the shape of the bar. For circular cross sections, one has:

$$\theta = \frac{T}{J\mu}, \tag{27}$$

where T is the torque and $J = 0.5 \cdot \pi r^4$ is the polar moment of inertia. For rectangular sections:

$$\theta = \frac{T}{Kab^3\mu}, \tag{28}$$

where a and b are the dimensions of the rectangle (with $a > b$) and K is a coefficient that depends of the ratio $\alpha = a/b$. Francu et al. [8] present the following formula to calculate K:

$$K(\alpha) = \frac{2^8}{\pi^6} \sum_{i \in \mathcal{N}} \sum_{j \in \mathcal{N}} \frac{\alpha^2}{i^2 j^2 (i^2 + \alpha^2 j^2)}, \tag{29}$$

$\mathrm{N}_I = \{1, 3, 5, 7, ...\}$. The values of K for some ratios α are in Table 1.

Table 1. The numerical values of β

α	1	1,5	2	3	4	5	6	8	10	∞
β	0,141	0,196	0,229	0,263	0,281	0,291	0,298	0,307	0,312	1/3

Murakami [9] gives an approximation for the angle of rotation for an L-section of height and width a, with thickness h, given by:

$$\theta = \frac{3T}{2ah^3\mu}. \tag{30}$$

The simulations were performed with the MATLAB ®software, using the FDA-MNCP algorithm (proposed by Gutierrez et al. [3]) to find the eq. (20) solution. For the physical parameters, standard values were adopted for structural steel named A-36 by ASTM (American Society for Testing and Materials) or MR-250 by ABNT (Brazilian Association of Technical Standards). According to Hibbeler [10], the modulus of elasticity for this steel is $E = 200\,GPa$, while the modulus of rigidity is $\mu = 75\,GPa$. The plasticity threshold used is $\gamma = 250MPa$, as defined in NBR 7007:2016, which describes the requirements for the use of carbon steel and high-strenght low-alloy steel for strutural use.

4.1 Different rectangular proportions

An interesting point of the rectangular case is to analyze how the variation in the proportion interferes in the plasticity regions. Figure 1 displays the results for different ratios k_1/k_2 with $c = 5$ and unit area. $N_2 = 40$ was fixed and N_1 varies proportionally to maintain the degree of refinement. The plastic percentages found were: (a) 23.27%, (b) 20.78% and (c) 15.08%.

Note that the plastic zones flatten towards the largest dimension, while they decrease and even disappear towards the smallest dimension. As previously shown, c depends on the angle of rotation, which in turn depends on the shape of the bar and the torque applied. Thus, if c is maintained even with section changes, a torque adjustment is implicitly imposed so that the resulting angle of rotation is the same. In this case, the torque is decreasing, which results in this decrease in the plastic regions.

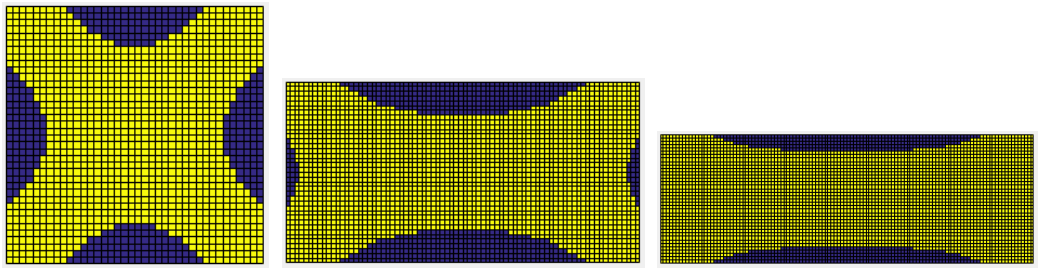

(a) $k_1/k_2 = 1$ (b) $k_1/k_2 = 2$ (c) $k_1/k_2 = 3$

Figure 1. Plastic zones (blue) for rectangular section with fixed area, $c = 5$

Now the torque will be maintained and c recalculated for each section variation. Considering the physical parameters, the area of the side square $10\,cm$ is fixed. Let $T = 85kNm$ and $N_2 = 40$, with N_1 varying proportionally, the Figure 2 presents the results. The following plastic percentages were obtained: (a) 22.16%, (b) 31.04% and (c) 40.68%. Comparing the regions obtained with Figure 1, it can be seen how the shape of the section actually has a huge impact on the angle of rotation. Adjusting c for each ratio change made the regions stay similar.

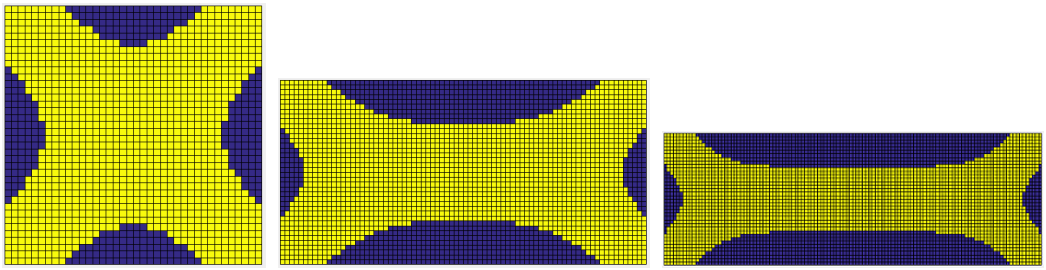

(a) $k_1/k_2 = 1;\ c = 48, 37$ (b) $k_1/k_2 = 2;\ c = 59, 47$ (c) $k_1/k_2 = 3;\ c = 77, 47$

Figure 2. Plastic zones (blue) for rectangular section with fixed area, calculated c

4.2 Formats circular, square and L

Figure 3 shows the results for cross sections of unit area in different shapes with fixed $c = 10$ and the following parameters (i) Square: $k_1 = 1$ and $N = 80$, (ii) Disk: $r = \sqrt{1/\pi}$ and $N_r = N_\theta = 80$, (iii) Section in L: $k_1 = 0.5$, $k_2 = 0.75$, $N_1 = 33$ and $N_2 = 49$. As discussed for the rectangular case, fixing c for different shapes implies different values of torque. As discussed for the rectangular case, fixing c for different shapes implies different values of torque. Therefore, a similar example was developed with T fixed and c calculated, taking the square side 10 cm as a reference for area. The following parameters were used: (i) Square: $k_1 = 0.1$ and $N = 80$, (ii) Disk: $r = \sqrt{0.01/\pi}$ and $N_r = N_\theta = 80$, (iii) Section in L: $k_1 = 0.05$, $k_2 = 0.075$, $N_1 = 33$ and $N_2 = 49$. The following parameters were used: (i) Square: $k_1 = 0.1$ and $N = 80$, (ii) Disk: $r = \sqrt{0.01/\pi}$ and $N_r = N_\theta = 80$, (iii) L-section: $k_1 = 0.05$, $k_2 = 0.075$, $N_1 = 33$ and $N_2 = 49$. Figure 4 shows the results obtained for $T = 200kNm$.

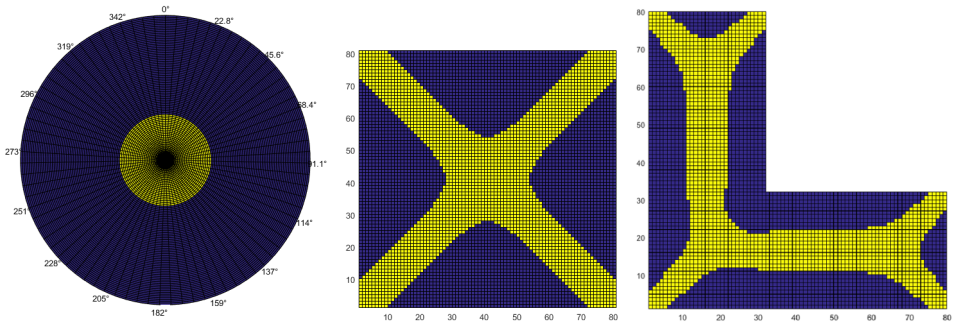

(a) Disk (b) Square (c) L-section

Figure 3. Plastic zones (blue) for different shapes with fixed area, $c = 5$

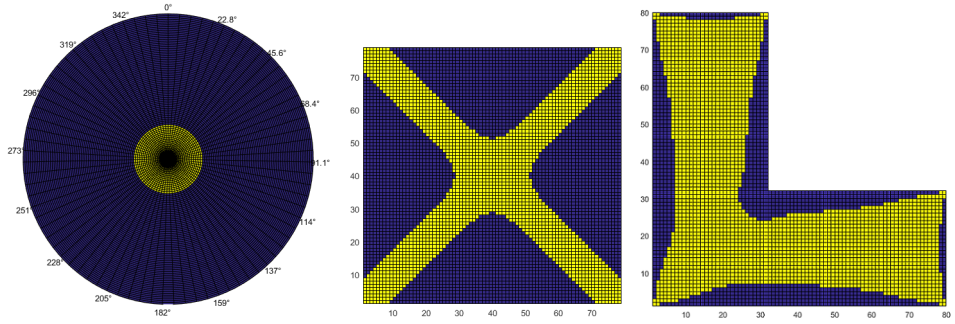

(a) Disk; $c = 100, 53$ (b) Square; $c = 113, 82$ (c) L-section; $c = 45, 51$

Figure 4. Plastic zones (blue) for different shapes with fixed area, calculated c

Table 2 shows a comparison of the plasticity area for each section, for fixed c and calculated c. There is a significant variation in the values for each case, but the circular section remains with the highest plastic percentage and the L-section with the smallest. Comparing the results obtained in Figures 3 and 4, one may observe that the

adjustment in c due to geometry generates a sharp drop in the size of the plastic regions for the L-section.

Table 2. The plastic percentages for different shapes with fixed area

Cross section	Plasticity, fixed c (%)	Plasticity, calculated c (%)
Disk	89,69	94,14
Square	58,41	63,77
L	53,95	27,98

5 Conclusions

In this work it was possible to observe how the shape of the cross section influences the plasticity areas. For the rectangular case, c calculated for the ratio $k_1/k_2 = 3$ represents an increase of more than 60% with respect to the c calculated for a square section of the same area. This reflects in higher plastic percentages, even with the shape of the regions being similar. As plasticity represents a permanent deformation, in general one wants the material to remain in the elastic phase. Therefore, as expected, the closer to the ratio $k_1/k_2 = 1$, the less the bar will suffer the effects of torsion. In the comparison between the three bar shapes, the L-section is much more resistant. However, it is important to highlight that the angle of rotation approximation proposed by Murakami [9] considers slender bars. For more conclusive results it would be necessary to further investigate the formulation of the angle θ.

Acknowledgements. The authors would like to thank the financial support provided by the Coordenação de Aperfeiçoamento de Pessoal de Nível Superior – Brasil (CAPES) for this research project.

Authorship statement. The authors hereby confirm that they are the sole liable persons responsible for the authorship of this work, and that all material that has been herein included as part of the present paper is either the property (and authorship) of the authors, or has the permission of the owners to be included here.

References

[1] E. D. Dolan, J. J. More, and T. Munson. Benchmarking optimization software with cops 3.0. *Mathematics and Computer Science Division*, 2004.
[2] H. Brezis and M. Sibony. Equivalence de deux inéquations variationnelles et applications. *Archive for Rational Mechanics and Analysis*, vol. 41, n. 4, pp. 254–265, 1971.
[3] A. E. R. Gutierrez, S. R. Mazorche, J. Herskovits, and G. Chapiro. An interior point algorithm for mixed complementarity nonlinear problems. *Journal of Optimization Theory and Applications*, vol. 175, n. 2, pp. 432–449, 2017.
[4] M. H. Sadd. *Elasticity: theory, applications, and numerics*. Academic Press, Cambridge, 2020.
[5] J. F. Rodrigues. *Obstacle problems in mathematical physics*. North-Holland, Rio de Janeiro, 1987.
[6] T. A. Danelon. Resolução numérica do modelo da torção elastoplástica via complementaridade mista para seção em l. *Proceeding Series of the Brazilian Society of Computational and Applied Mathematics*, vol. 8, *in press*.
[7] M. C. Lai. A note on finite difference discretizations for poisson equation on a disk. *Numerical Methods for Partial Differential Equations*, vol. 17, n. 3, pp. 199–203, 2001.
[8] J. Francu, P. Novackova, and P. Janicek. Torsion of a non-circular bar. *Engineering Mechanics*, vol. 19, n. 1, pp. 45–60, 2012.
[9] Y. Murakami. *Theory of elasticity and stress concentration*. John Wiley & Sons, Chichester, 2017.
[10] R. C. Hibbeler. *Resistência dos materiais*. Pearson Prentice Hall, São Paulo, 2004.